

## THE MATHEMATICAL MODEL OF A COLD CRUCIBLE

KAZUHIKO IWAI, MAMORU KUWABARA, KENSUKE SASSA, AND SHIGEO ASAI  
Department of Materials Processing Engineering, Faculty of Engineering,  
Nagoya University, Furo-cho, Chikusa-ku, Nagoya, 464-01, Japan

### ABSTRACT

Three theoretical models are developed to estimate the effects of design parameters of a cold crucible. The first one is a lumped parameter model, the concept of which is based on the principle of a transformer, and which is easier to calculate than the other two models. The second is a filiform wire model which is an axisymmetrical three-dimensional model based on a magnetic potential method. The third is a strict three-dimensional model where the boundary element method is applied to solve the magnetic field distribution around a cold crucible system.

### 1. INTRODUCTION

Induction melting of conductive solids has been applied widely to refine or to cast the materials. However, the conventional induction melting is based mainly on the utilization of the ohmic dissipation to heat the materials and the electromagnetic body force to stir the melt in a crucible. Thus, in the conventional induction melting, we can not avoid the chemical and mechanical contaminations of melt from a refractory or a crucible. Effective utilization of the third electromagnetic function representing magnetic stress acting on a surface of the melt enables one to maintain the charge without any contact with the crucible and induction coil. One such example is the levitation melting.

However, its application is limited to fusing a small amount of material. An alternative way of utilizing the third function is the cold crucible[1] (Fig.1) composed of a segmented and water-cooled copper mold which can transmit the magnetic energy of a coil effectively to a charge inside the crucible. Since the charge is electrically repelled from the neighboring conductive mold, the charge is allowed to melt and solidify within the mold without any contact with the mold. Then the cross-sectional shape of the

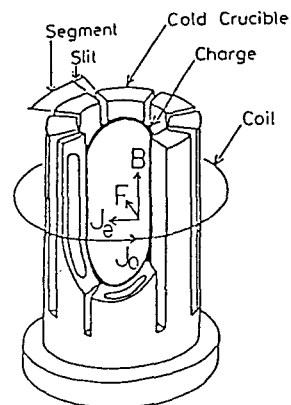


Fig.1

Schematic view of a cold crucible

solidified ingot would be prescribed by the inner configuration of the mold. Thus, the cold crucible is an attractive system for remelting and casting chemically reactive and/or high melting-point materials with minimum contamination.

In this paper, three different mathematical models for a cold crucible are developed to evaluate the effects of design parameters on the heat generation rates in the charge and the crucible and on the magnetic field around a continuous casting type of a cold crucible. The magnetic field predicted by the three dimensional model has been compared with that measured and the heat generation rates predicted by the lumped model have been compared with experimental results.

## 2. LUMPED PARAMETER MODEL

### 2.1. The evaluation of heat generation rate

Delage et al.[2],[3] presented a lumped parameter model, based on the concept of a transformer, where an induction coil corresponds to the primary winding and the combination of the crucible and the charge corresponds to the secondary winding. The present model is an extension of the model developed by Delage et al.[2],[3]. The concept of the extended model is shown in Fig.2. The coil current induces an eddy current on the outer surface of the crucible which turns into the inner surface of the crucible following the conservation principle of electric charges. Then the current on the inner surface of the crucible induces an eddy current in the molten charge.

The relationships between the voltage  $V$  and current  $I$  in each position are given by

$$V_1 = R_1 I_1 + j\omega (L_1 I_1 + M_{12} I_2) \quad (1)$$

$$V_2 = -R_2 I_2 - j\omega (L_2 I_2 + M_{12} I_1) \quad (2)$$

$$V_3 = R_3 I_3 + j\omega (L_3 I_3 + M_{34} I_4) \quad (3)$$

$$V_4 = R_4 I_4 + j\omega (L_4 I_4 + M_{34} I_3) \quad (4)$$

$$V_2 = V_3 \quad (5)$$

$$I_2 = I_3 \quad (6)$$

$$V_4 = 0 \quad (7)$$

where  $j$  : imaginary unit,  $L$  : self inductance,  $M$  : mutual inductance,  $R$  :

resistance,  $\omega$  : angular frequency, and subscript 1,2,3 and 4 represent coil, outer and inner surfaces of the crucible, and charge, respectively.

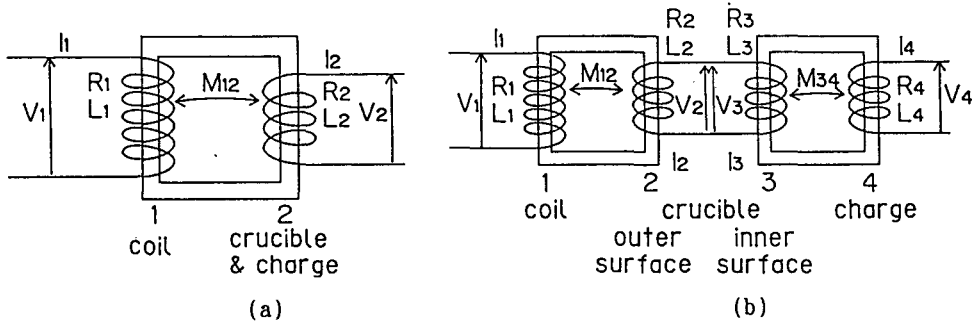


Fig.2 Concepts for Delage's model (a) and the present model (b)

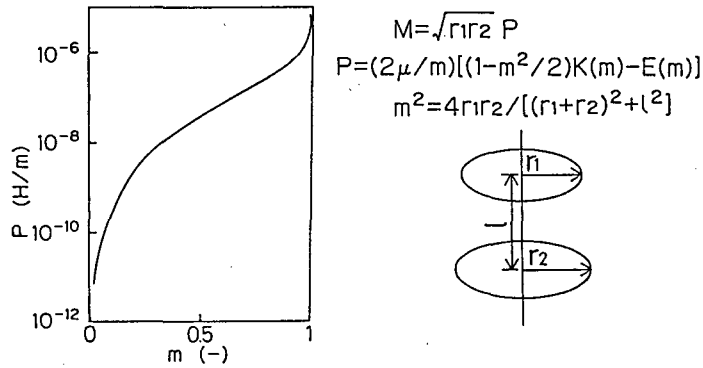


Fig.3 The mutual inductance between two coaxial loops

When a high frequency current is used, the resistance is negligible small in comparison with the reactance. Through some manipulations of Eqs. (1)to(7), the relationship between currents are derived as follows:

$$I_2 = - \{M_{12}L_4 / \{L_4(L_2+L_3) - M_{34}^2\}\} I_1 \quad (8)$$

$$I_4 = \{M_{12}M_{34} / \{L_4(L_2+L_3) - M_{34}^2\}\} I_1 \quad (9)$$

Equations(8) and (9) tell that if the self inductance, L and the mutual inductance, M are estimated, the eddy currents in the crucible and the charge can be calculated. If the crucible and the charge are so sliced in the perpendicular direction to the axis as to image several loops of currents, the mutual inductance between two conductors can be easily evaluated. The mutual inductance between two coaxial circular loops with a geometrical configuration as given in Fig.3 is expressed as follows:

$$M = (2\mu/m)(\sqrt{r_1 r_2}) \{ \{1-(m^2/2)\}K(m)-E(m) \} = \sqrt{r_1 r_2} P \quad (10-a)$$

$$P = (2\mu/m) \{ \{1-(m^2/2)\}K(m)-E(m) \} \quad (10-b)$$

$$m^2 = 4r_1 r_2 / \{ (r_1 + r_2)^2 + \varrho^2 \} \quad (10-c)$$

where  $r_1$  and  $r_2$  : radii of loops,  $\varrho$  : the distance between loops,  $\mu$  : magnetic permeability, and  $K$  and  $E$  : the first and second kinds of complete elliptic integrals, respectively. When the numbers of the sliced loops in two conductors are  $n_1$  and  $n_2$ , the mutual inductance between two loops is given by

$$M = \sum_{i=1}^{n_1} \sum_{j=1}^{n_2} M_{ij} \quad (11)$$

Finally, the heat generation rates in the charge and the crucible can be obtained by

$$Q_{ch} = n_{ch} R_{ch} I_1^2 \quad (12)$$

$$Q_{cr} = n_{cr} R_{cr} I_2^2 \quad (13)$$

where  $Q$  : heat generation rate,  $n$  : the number of current loops, and subscript  $ch$  and  $cr$  represent the charge and the crucible, respectively. The resistance,  $R$ , is evaluated by

$$R = 2\pi r / (\sigma \delta \Delta h) \quad (14)$$

where  $\delta$  : skin depth,  $\Delta h$  : height of sliced loop and  $\sigma$  : electric conductivity

## 2.2. Result

In order to verify the accuracy of the model, heat generation rates in the charge and the crucible in a cold crucible system are compared with the observed results. The configuration of the system is illustrated in Fig.4. The size of the aluminium stick corresponding to the charge is  $\phi 38\text{mm} \times \varrho 110\text{mm}$ . The copper crucible has eight slits with a depth of 100mm, 40mm I.D., 76mm O.D., and a height is 140mm. The 4 turn induction coil having a 10mm $\times$ 15mm tetragonal cross section is adjusted to get the same head position with the charge and the crucible. The charge and the crucible are cooled by water. Then the heat generation rates are evaluated by measuring the temperature differences between the inlet and outlet of the

cooling water. The imposed current in the coil was 1200A at maximum and 20kHz.

The results are shown in Fig.5. Heat generation rates in the charge calculated by this model are in closer agreement with the measurements than those by the model of Delage et al.[2],[3]. The heat generation rates in the crucible are underestimated by this model and overestimated by the model of Delage et al.[2],[3].

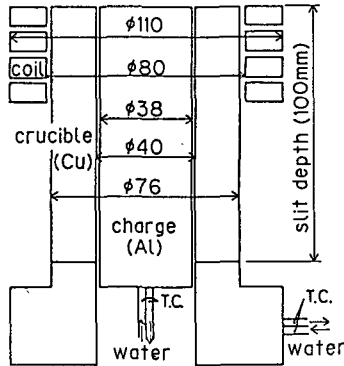


Fig.4 Experimental system for measuring heat generation rates

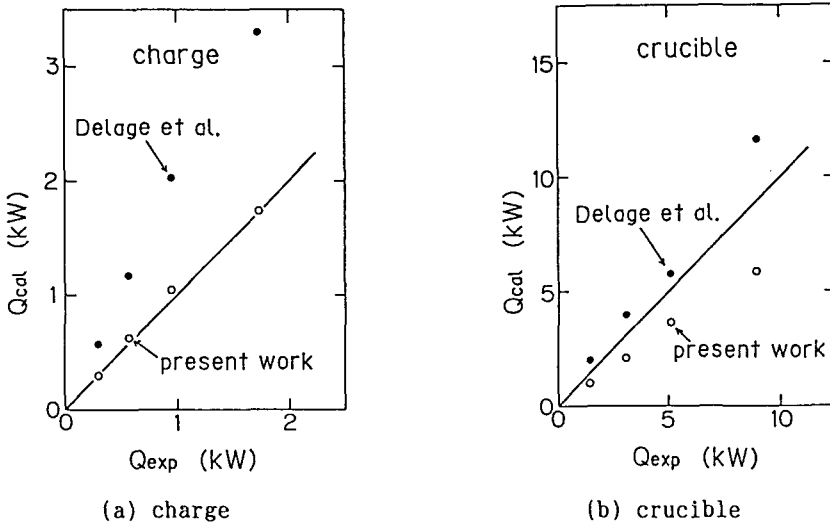


Fig.5 Comparisons of heat generation rates by calculations and experiments

The discrepancy between the calculated values by the present model and the experimental results is attributed to the evaluation of the eddy current which was not taken into account in the non-slit and flange parts of the crucible.

### 3. FILIFORM WIRE MODEL

#### 3.1. Formulation

The eddy current density  $J_e$  is related to the magnetic vector potential  $A$  as follows:

$$J_e = -\sigma (\partial A / \partial t) - \sigma \nabla \phi \quad (15)$$

where  $t$  : time, and  $\phi$  : electric scalar potential.

The conductor is now assumed to be composed of a set of horizontal current loops which are of finite depth and height and are mutually isolated. Then the term  $\nabla \phi$  giving a criterion of the electric field due to the eddy current may be disregarded. In addition, the sinusoidal time variation with an angular frequency  $\omega$  is assumed. Equation(15) then reduces to

$$J_k = -j \sigma \omega A_k \quad (16)$$

where  $A_k$  stands for the total vector potential at the  $k$ -th elementary loop. It can be evaluated, as shown later in Eq.(20), by a linear function of the entire known and unknown current densities including  $J_k$  on the loop just concerned. Simultaneous solution of Eq.(16) applied to the entire elementary loops gives the self-consistent solution for  $J_k$  and thus distributions of the vector potential and the magnetic field in space.

The  $i$ -th elementary loop of radius  $\rho$  centered about ( $r=0, z=\xi$ ) is carrying a current  $I_i$ . Then the magnetic vector potential at a spatial position  $P(r,z)$  with constant permeability  $\mu$  can be found on the basis of the Biot-Savart's law given by Eq.(17), which has only one circumferential direction  $A_\theta$

$$A_{P,i} = (\mu / \pi) I_i f_{P,i} \quad (17)$$

where  $f_{P,i}$  is a dimensionless function represented the first and second kinds of complete elliptic integrals expressed by  $K$  and  $E$ , respectively, and is given by

$$f_{P,i} = (1/m) \sqrt{\rho/r} \{ (1-m^2/2)K(m) - E(m) \} \quad (18-a)$$

$$m^2 = 4\rho r / \{ (r + \rho)^2 + (z - \xi)^2 \} \quad (18-b)$$

In the case of an incremental circular conductor of vertical thickness  $\Delta h$ , the induced current whose amplitude is exponentially decaying toward inside may be integrated over a sufficient depth to yield the  $i$ -th loop current  $I_i$  to give

$$I_i = J_i (\Delta h) \delta / (1+j) \quad (19)$$

where  $J_i$  designates the surface current density of the  $i$ -th loop.

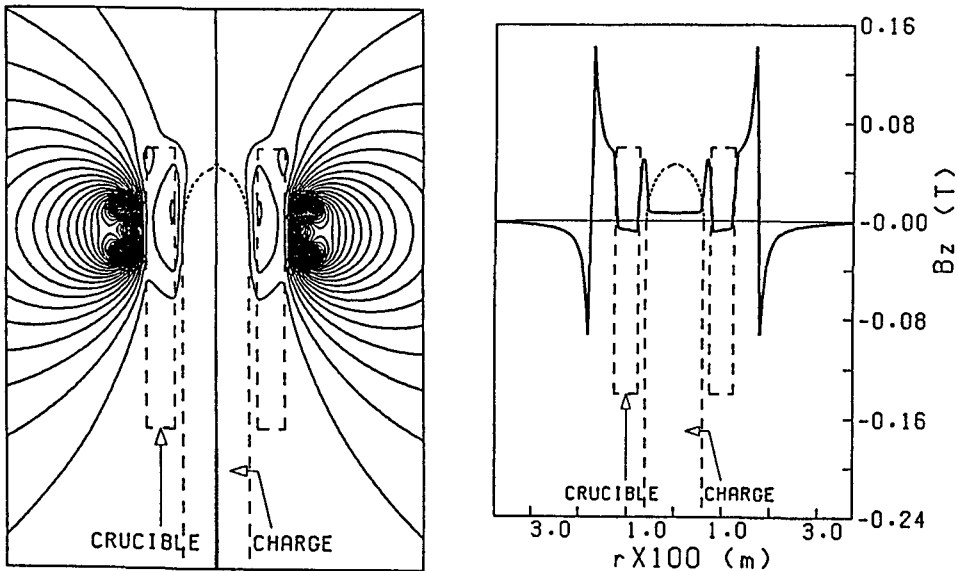
The total vector potential at the position P is found by integrating the contribution from all the incremental elements as:

$$A_P = \sum_{j=1}^{n_s} \sum_{i=1}^n A_{P,ij}(\text{Crucible}) + \sum_{i=1}^n A_{P,i}(\text{Charge}) + \sum_{i=1}^{n_{coil}} A_{P,i}(\text{Coil}) \quad (20)$$

where  $n$ ,  $n_s$ ,  $n_{coil}$  are the number of incremental loops, numbers of segments, and winding turns of coil, respectively. It should be noted in Eq.(20) that the summation is made for every component of the vector potential due to each elementary loop. It is noted furthermore that Eq.(20) is still valid to evaluate  $A_k$  in Eq.(16) by specifying the position P on the  $k$ -th elementary loop of interest.

Since we now consider only one slit case, the elementary loops are all coaxial and only the circumferential component of A exists.

The position of the free boundary of melt which interacts with the magnetic field should be determined on the basis of a static equilibrium of the hydrostatic pressure, the surface tension and the magnetic pressure acting on it.



(a) magnetic field lines

(b) radial distributions of  $B_z$

Fig.6 Computed results by using of filiform wire model

### 3.2. Results

The cold crucible system computed is a continuous casting type. The dimensions of the crucible was 30mm I.D., 50mm O.D. and 100mm in height. This crucible had six radial slits with a vertical depth of 90mm and with a slit clearance of about 5mm. An induction coil having a diameter of 12mm is spirally wound around the crucible with a pitch of 10mm ,and located 20mm and 30mm below the top of the crucible. The coil carried a high frequency current of 2800A and 1800Hz.

Figure 6 is the computed results with respect to (a):the magnetic flux lines as contour lines of  $rA_\theta$  , and (b):radial distribution of  $B_z$ . We can find an intensified magnetic flux density in the space between the crucible and the charge, which is responsible for counteracting the hydrostatic pressure of melt.

### 4. THREE DIMENSIONAL MODEL

There are various methods such as FEM(Finite Element Method), BEM(Boundary Element Method), FDM(Finite Difference Method) to compute three dimensional electric and magnetic fields. When employing FEM or FDM, we must divide all of the region to be analyzed into elements, and each element or node has at least three unknown variables to be solved. When using BEM, however elements exist only on the boundary so that the number of unknown variables are much fewer than that in FEM or FDM. Another substantial advantage of BEM is that an infinitely extending variable such as electric and magnetic field can be treated in a finite compact region. Thus, BEM was selected for the present work.

#### 4.1. Formulation

Governing equations are Maxwell's equations (21)to(23) and Ohm's law (24).

$$\mathbf{J} = (1/\mu)(\nabla \times \mathbf{B}) \quad (21)$$

$$\nabla \times \mathbf{E} = -(\partial \mathbf{B} / \partial t) \quad (22)$$

$$\nabla \cdot \mathbf{B} = 0 \quad (23)$$

$$\mathbf{J} = \sigma \mathbf{E} \quad (24)$$

where  $\mathbf{B}$  : magnetic flux density,  $\mathbf{E}$  : electric field, and  $\mathbf{J}$  : current density. From Eqs.(21) to (24) and the assumption of sinusoidal time

dependence of magnetic field, the partial differential equation for B is derived as follows:

$$\nabla^2 \mathbf{B} - j\omega \mu \sigma \mathbf{B} = 0 \quad (25)$$

This is the governing equation for conductive region. Furthermore in non-conductive region, the second term of the left-hand side of Eq.(25) is zero so that the governing equation for the current free region reduces to Eq.(26).

$$\nabla^2 \mathbf{B} = 0 \quad (26)$$

Green's theorem is used to get the following boundary integral form of the governing equations:

$$c_k B_i = \int_S \{ \phi (\partial B_i / \partial n) - B_i (\partial \phi / \partial n) \} dS \quad (27)$$

$$\text{where } \phi = e^{-jkr} / 4\pi r, \quad k = \sqrt{-j\omega \mu \sigma}$$

and  $B_i$  : each component of  $\mathbf{B}(B_x, B_y, B_z)$ ,  $c_k$  : the solid angle subtended by S at computation point,  $r$  : the distance between the source point and the computation point,  $S$  : the boundary of the region to be analyzed,  $\phi$  : the fundamental solution, and  $\partial/\partial n$  is derivative to the normal of the surface. As no magnetic material exists in the region of interest, the boundary conditions are written as follows:

$$B_i |_{\text{region I}} = B_i |_{\text{region II}} \quad (28-a)$$

$$(\partial B_i / \partial n) |_{\text{region I}} = -(\partial B_i / \partial n) |_{\text{region II}} \quad (28-b)$$

The set of Eq.(27) has to be simultaneously solved under the conditions of Eq.(28).

#### 4.2. Results

The system for analysis is almost the same as that for filiform wire model except the charge. The frequency of coil current is relatively high(1800Hz) so that the current flows only on the surface. Then the region to be solved is all the space except the interior of the coil. We assume that the charge deformation due to magnetic pressure is negligible. Only one fourth of the entire space composed of the two and a half segments is analyzed on the basis of the symmetry. 729 triangular elements are adopted in the computation.

The comparison of the computed and measured values of  $B_z$  along the axial

direction in a slit region is shown in Fig.7. The overall agreement is satisfactory. The distributions of magnetic field over two vertical planes are shown in Fig.8. Magnetic field rotates around an induction coil. In the crucible and the charge, magnetic field decays and its direction differs from that in the surrounding. We can see that on the surface of the crucible facing the coil, the direction of the magnetic field vector is opposite to that of the coil.

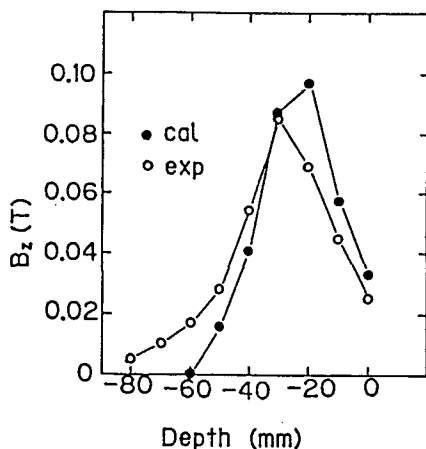
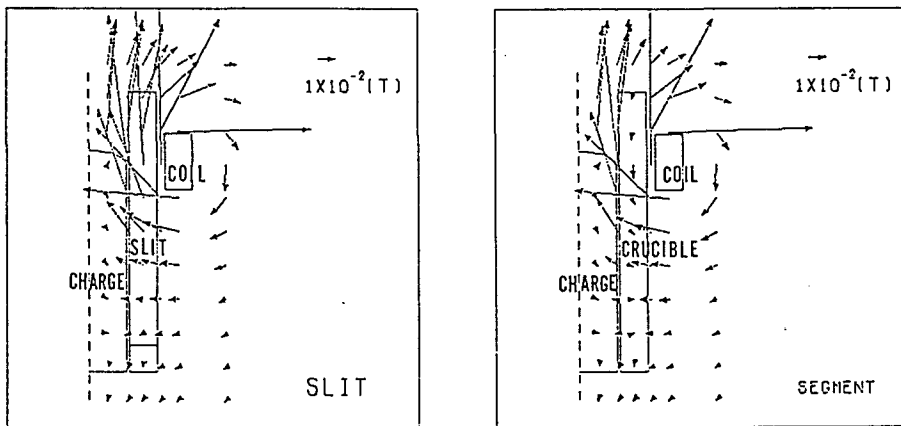


Fig.7 Comparison of  $B_z$  in a slit by calculation and experiment



(a) slit section

(b) segment section

Fig.8 Spatial distribution of  $B$  over vertical section of the system

## 5. CONCLUSIONS

Three theoretical models are developed to estimate the effects of design parameters of a cold crucible on the heat generation rates in a charge and a

crucible or on the magnetic field. The lumped parameter model which is similar to a transformer is suitable for estimating heat generation rate. The filiform wire model is an axisymmetrical three-dimensional model based on a magnetic potential method, which allows to combine with thermal analysis. The boundary element method is applied to solving three-dimensional magnetic field and offers more precise and useful information than the others but requires a great deal of computation cost and time.

#### REFERENCES

1. Siemens and Halske A.G.: German Pat. 518.499, Jan.19., 1931.
2. D. Delage, R.Ernst and J.Driole, IEEE.Trans, on Industrials Applications, (1982)
3. D. Delage, R.Ernst and J.Driole, Proc.Symp.IUAM. Cambridge, (1982) p108.